Bioorganic & Medicinal Chemistry 18 (2010) 1749–1760

Contents lists available at ScienceDirect

Bioorganic & Medicinal Chemistry

journal homepage: www.elsevier.com/locate/bmc

Targeting Alzheimer's disease: Novel indanone hybrids bearing a pharmacophoric fragment of AP2238

Stefano Rizzo [a], Manuela Bartolini [a], Luisa Ceccarini [a], Lorna Piazzi [a], Silvia Gobbi [a], Andrea Cavalli [a,b], Maurizio Recanatini [a], Vincenza Andrisano [a], Angela Rampa [a,*]

[a] Department of Pharmaceutical Sciences, University of Bologna, Via Belmeloro 6, 40126 Bologna, Italy
[b] Department of Drug Discovery and Development, Italian Institute of Technology, Via Morego 30, 16163 Genova, Italy

ARTICLE INFO

Article history:
Received 10 September 2009
Revised 22 January 2010
Accepted 29 January 2010
Available online 4 February 2010

Dedicated to Professor Piero Valenti on the occasion of his 70th birthday

Keywords:
Alzheimer's disease
AChE
Aβ inhibition
Indanone
Hybrid molecules

ABSTRACT

We report on a series of hybrid compounds structurally derived from donepezil and AP2238. This study was aimed at improving the activities of the reference compounds, donepezil and AP2238, and at broadening the range of activities of new derivatives as, due to the multifactorial nature of AD, molecules that modulate the activity of a single protein target are unable to significantly modify the progression of the disease. In particular, the indanone core from donepezil was linked to the phenyl-*N*-methylbenzylamino moiety from AP2238, through a double bond that was kept to evaluate the role of a lower flexibility in the biological activities. Moreover, SAR studies were performed to evaluate the role of different substituents in position 5 or 6 of the indanone ring in the interaction with the PAS, introducing also alkyl chains of different lengths carrying different amines at one end. Derivatives **21** and **22** proved to be the most active within the series and their potencies against AChE were in the same order of magnitude of the reference compounds. Compounds **15**, **21–22**, with a 5-carbon alkyl chain bearing an amino moiety at one end, better contacting the PAS, remarkably improved the inhibition of AChE-induced Aβ aggregation with respect to the reference compounds. They also showed activity against self-aggregation of $A\beta_{42}$ peptide, the most amyloidogenic form of amyloid produced in AD brains, while the reference compounds resulted completely ineffective.

1. Introduction

It is known that Alzheimer's disease (AD) is a multifactorial disorder involving the malfunction of different, but related, biochemical pathways in which certain proteins play a key role. A significant alteration of cholinergic markers,[1,2] together with extraneuronal deposition of β-amyloid (Aβ) plaques, are the most significant hallmarks depicting the pathology.[3,4] In particular, because of an altered catabolism of the so called 'amyloid precursor protein' (APP), small insoluble peptides are formed that undergo aggregation into senile plaques, either spontaneously or through induction by chaperone molecules such as acetylcholinesterase (AChE). In fact, it has been shown that AChE, besides its catalytic function, can also bind to Aβ and act as a promoter of Aβ fibril formation.[5] This action was associated with the peripheral anionic site (PAS) located at the lip of the enzyme's gorge and several ligands that bind to this site have been shown to retard aggregation.[6,7] On the other hand, growth of the fibrils occurs by assembly of the Aβ seeds into intermediate protofibrils, which in turn self-associate to form mature fibers, and thus compounds that are able to slow or block the amyloid polymerization process could be considered potential drugs for AD. To date, no available treatment is known to stop the progression of AD, and currently approved drugs (including donepezil, Fig. 1) only seem to act as palliative by temporary ameliorating cognitive impairment.[8] Moreover, it is widely accepted that targeting different biological entities, involved in the same pathology, can be a better strategy to block the course of multifactorial diseases rather than just reducing their symptoms. For this reason, designing molecular entities able to address more than one disease-related target has now become a challenging and interesting approach in the drug design for multifactorial diseases such as AD.

Our research group has been involved through the years in the development of AChE inhibitors aimed at inhibiting ACh degradation, and recently focused the efforts on the design and synthesis of dual-binding AChE inhibitors, that simultaneously inhibit AChE and AChE-induced Aβ aggregation.[9–12] In particular, AP2238 was the first published compound,[9] designed to bind both anionic sites of the human acetylcholinesterase (hAChE) for which the simultaneous inhibition of the catalytic and the amyloid-β pro-aggregating activities of AChE was verified. The potency of AP2238 against AChE is comparable to that of donepezil, while its ability to contrast Aβ aggregation is higher. Docking studies of AP2238 at the

* Corresponding author. Fax: +39 051 2099734.
E-mail address: angela.rampa@unibo.it (A. Rampa).

0968-0896/$ - see front matter © 2010 Elsevier Ltd. All rights reserved.
doi:10.1016/j.bmc.2010.01.071

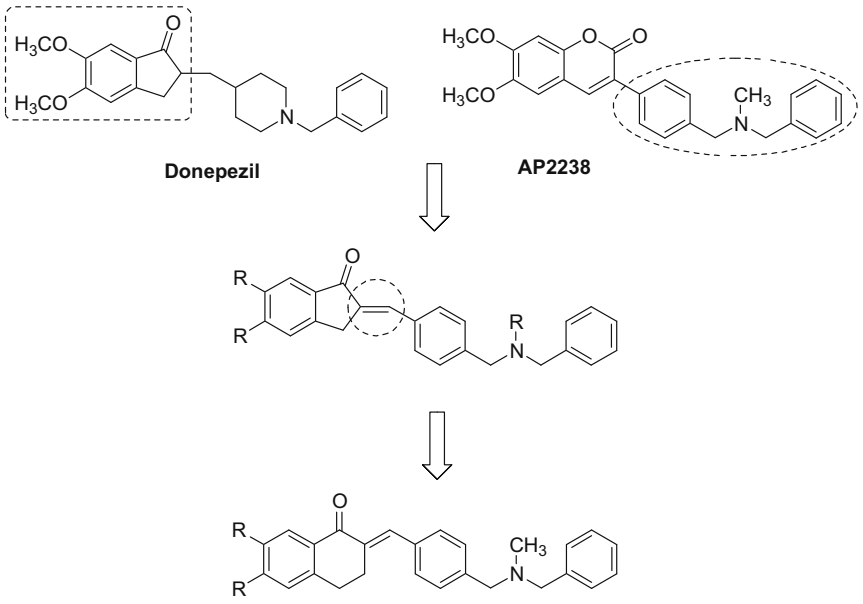

Figure 1. Design of target molecules.

hAChE gorge have shown that its benzyl group interacted by means of a π–π stacking with the indole ring of Trp86; the spacer phenyl ring could establish both a π–π interaction with the phenol ring of Tyr341 and an OH-π interaction with the hydroxyl group of Tyr124; the protonated amino group was involved in a cation-π interaction with the phenol ring of Tyr337; the carbonyl group of the coumarin moiety and eventually the endocyclic oxygen could establish H-bond interactions with the backbone amide group of Phe295; the aromatic moiety of the coumarin ring interacted with Trp286, by means of a π-π stacking.[9] Indeed, AP2238 contacted the catalytic site of hAChE and apparently it reached the PAS of the enzyme (Trp286 and surrounding residues) better than donepezil.

Here, we report on a series of hybrid compounds structurally derived from donepezil and AP2238. In particular, as depicted in Figure 1, the indanone core from donepezil was linked to the phenyl-*N*-methylbenzylamino moiety from AP2238, to maintain the additional OH-π interaction with Tyr124, through a double bond that was kept to evaluate the role of a lower flexibility in the biological activities. Moreover, SAR studies were performed to evaluate the role of different substituents in positions 5 or 6 of the indanone ring in the interaction with the PAS. In particular, since 6-substituted derivatives turned out to be the most promising compounds, we further modified this position by introducing alkyl chains of different lengths carrying different amines at one end, with the purpose to mime the diethylmethylammoniumalkyl moiety of propidium, a potent PAS ligand.[7] A derivative in which the phenyl-*N*-methylbenzylamino moiety from AP2238 was replaced by a phenyl-*N*-ethylbenzylamino group was synthesized as well, like AP2243.[11] Furthermore, the indanone ring itself was replaced by a tetralone scaffold. As a result, 22 new compounds were synthesized and tested for their biological activities toward hAChE and human butyrylcholinesterase (hBuChE). Among them, a group of selected inhibitors was also tested for the inhibition of both AChE-induced and self Aβ aggregation.

2. Chemistry

The synthesis of the studied compounds was accomplished as shown in Scheme 1. Benzylic bromination with *N*-bromosuccinimide (NBS) of the commercially available 4-methylbenzonitrile afforded **23**, which was subsequently reacted with *N*-methylbenzylamine or *N*-ethylbenzylamine to afford amino derivatives **24** or **25**, respectively. These latter were oxidized using the Ni/Raney alloy to give aldehydes **26**–**27**, which were then reacted with the selected indanone or tetralone ring to give compounds **1–5** and **18**–**20**, respectively, via the aldol condensation. The synthesis of derivatives carrying substituents other than methoxy started by the selected commercially available hydroxy indanone or tetralone, that underwent alkylation with 1-bromo-ω-chloroalkanes or ω-dibromoalkanes (according to commercial availability) in the presence of K_2CO_3 affording aloalkyloxy derivatives **28a–c**, **29a**–**f**, and **30d**, which were subsequently condensed with aldehyde **26** to give **31a–c**, **32a–f** and **33d**. The ω-chloroalkyl derivatives **31a–c**, **32a–e** and **33d** were treated with NaI in refluxing methylethyl ketone to give the corresponding iodo-derivatives **34a**–**c**, **35a–e**, **36d**, and then subjected to nucleophilic substitution reaction by the selected amine to give the desired compounds **6–17** and **21–22**.

3. Enzyme inhibition

The inhibitory activity against AChE of the newly synthesized compounds was studied using the method described by Ellman[13] to determine the rate of hydrolysis of acetylthiocholine in the presence of the inhibitor. The selectivity of the compounds was also tested by determining their inhibitory activity against hBuChE. Some compounds, rationally selected, were also tested for their ability to prevent the hAChE-induced Aβ aggregation by a ThT-based fluorescence assay. Moreover, in view of enlarging their spectrum of action, the same series of selected compounds were in vitro evaluated for their capability of inhibiting β-amyloid self-aggregation.

4. Results and discussion

The inhibitory activities against both human recombinant AChE and BuChE from human serum of new derivatives, together with those of donepezil and AP2238 taken as references, are reported in Tables 1 and 2, and are expressed as IC_{50} values.

It was previously proven that methoxy substituents could improve the ability of the compounds to interact with the PAS, as for both inhibitors donepezil[14] and AP2238.[9] With regard to the

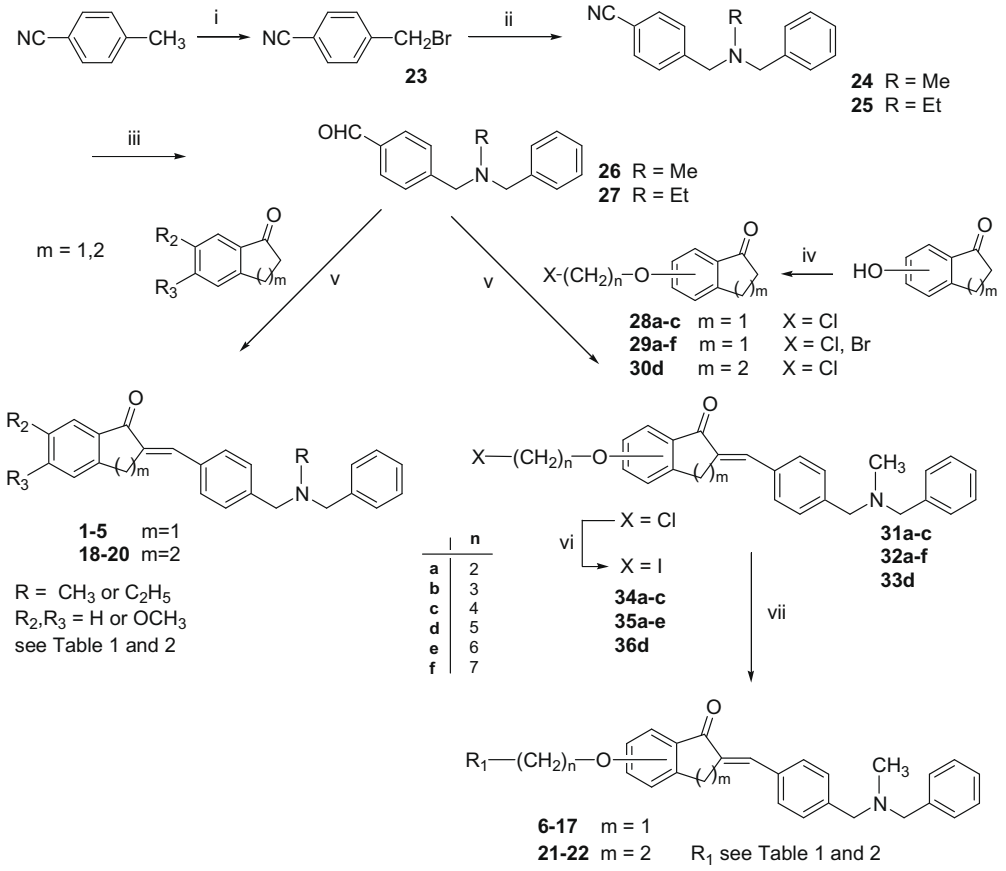

Scheme 1. Synthesis of the studied compounds. Reagents and conditions: (i) NBS, CCl_4, reflux; (ii) *N*-benzyl-*N*-methylamine or *N*-benzyl-*N*-ethylamine, toluene, reflux; (iii) Ni/Raney, HCOOH, reflux; (iv) $Br(CH_2)_nCl$, K_2CO_3, acetone, reflux; (v) NaOH, EtOH, rt; (vi) NaI, EtCOMe, reflux; (vii) selected amine, toluene, reflux.

role of the methoxy substituents in this new series, it can be noticed that, when placed in position 6 of the indanone ring, the methoxy group conferred a good activity (**3**, Table 1), while when it was moved to position 5, it led to a reduction in activity of two order of magnitude. These results are in agreement with those shown by the 5,6-dimethoxy derivative **1**, which is two times less active than compound **3**. The role of the methoxy group in position 6 appeared to be crucial in the interaction with the enzyme, as evicted by the lower activity (10 times less) of compound **5**, whose indanone ring does not carry any methoxy substituent, when compared with **3**. By analyzing Table 1, a detrimental effect on the biological activity can be noticed when the methyl substituent at the nitrogen was replaced by the homologous ethyl residue (compound **4**). A completely reversed trend was observed within the tetralone derivatives series, mono-methoxy substituted compounds being 10 times less active than the dimethoxy substituted compound **20** (Table 2).

To confirm the effective AChE binding mode of some representative novel AChE inhibitors here reported, **2**, **3**, **18**, and **19** underwent molecular modeling studies. Docking simulations were carried out with the software GOLD[15] and outcomes were rationalized by means of the clustering algorithm AClAP.[16,17] In Figure 2, the binding modes of **2**, **3**, **18**, and **19** are reported. It can be seen that all molecules could favorably interact with both the catalytic pocket and the PAS of the enzyme. In particular, the following major interactions, responsible for the inhibiting profiles of the selected molecules, could be identified: (i) the benzyl group of all the inhibitors interacts by means of π–π stacking with the indole ring of Trp86; (ii) the common spacer phenyl ring can establish a π–π interaction with the phenol of Tyr341, an OH-π interaction[18] with the hydroxyl group of Tyr124, and a T-shaped interaction with the side chain of Phe338; (iii) the protonated amino group of all inhibitors is involved in a cation-π interaction with the phenol ring of Tyr337; the bicyclic aromatic moiety (indanone of **2** and **3**, and tetralone of **18** and **19**) interacts with Trp286 by means of a π-π stacking; iv) the carbonyl group (shared by all the docked inhibitors) can establish H-bond interactions with the backbone amide groups of Phe295 and Arg296. Furthermore, we investigated the role of the methoxy group, which apparently did not specifically interact with AChE residues. Quantum chemical calculations carried out at the density functional level of theory (DFT) demonstrated that such a substituent could affect the H-bond between the carbonyl group and Phe295 and Arg296 backbones by means of a mesomeric effect. In particular, DFT calculations showed that the H-bonds of **18** (a 6-methoxy derivative) were about 0.5 kcal/mol more stable than H-bonds between **19** (the 7-methoxy derivative) and Phe295 and Arg296 backbones. Notably, as shown in Figure 1, the two molecules presented a very similar binding mode, and therefore the slight difference in biological activities here observed (Table 2) could be due to an electronic contribution to the carbonyl involved in the above mentioned H-bond interactions. Furthermore, the methyl group of the methoxy substituent was found to be at hydrophobic distance with the side chain of Leu289, and therefore it contributes to the overall interaction energy by means of a slight hydrophobic interaction. Such an interaction was conversely not possible for **2** (Table 1) that points the methoxy group in a rather different region when compared to the others. This could help explaining the remarkably lower activity of **2** when compared to **3**, **18** and **19**.

Methoxy substituents were also replaced by an alkyloxy chain bearing a diethylamino moiety at one end, to evaluate the role of

Table 1
Inhibitory activity on human AChE and BuChE, IC_{50} ratio of the studied compounds

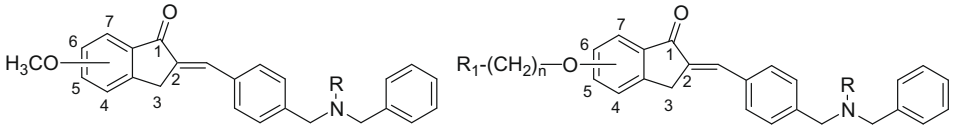

1-5 **6-17**

Compd	*n*	OCH_3 or chain position	R	R_1	IC_{50} hAChE (μM) ± SEM[a]	IC_{50} hBuChE (μM) ± SEM[a]	Ratio IC_{50} BuChE/AChE
1	—	5,6	CH_3	—	1.14 ± 0.05	144 ± 23	126
2	—	5	CH_3	—	28.7 ± 2.2	21.1 ± 26	0.73
3	—	6	CH_3	—	0.63 ± 0.05	7.93 ± 1.18	12.6
4	—	6	C_2H_5	—	4.93 ± 0.28	98.1 ± 4.5	19.9
5	—	—	CH_3	—	11.7 ± 1.1	29.9 ± 1.0	2.55
6	2	5	CH_3	NEt_2	2.90 ± 0.21	22.5 ± 3.9	7.76
7	3	5	CH_3	NEt_2	1.61 ± 0.35	11.4 ± 0.8	7.08
8	4	5	CH_3	NEt_2	3.95 ± 0.47	22.9 ± 1.6	5.80
9	2	6	CH_3	NEt_2	1.53 ± 0.07	11.9 ± 0.5	7.77
10	3	6	CH_3	NEt_2	1.32 ± 0.10	11.9 ± 0.7	9.01
11	4	6	CH_3	NEt_2	0.89 ± 0.15	3.52 ± 0.04	3.95
12	4	6	CH_3		0.89 ± 0.08	99.8 ± 5.3	112
13	4	6	CH_3		0.18 ± 0.02	10.0 ± 0.3	55.5
14	5	6	CH_3	NEt_2	0.19 ± 0.01	2.70 ± 0.15	14.2
15	5	6	CH_3		0.20 ± 0.02	7.70 ± 0.27	38.5
16	6	6	CH_3	NEt_2	0.38 ± 0.02	20.5 ± 1.8	53.9
17	7	6	CH_3	NEt_2	0.51 ± 0.03	33.0 ± 3.0	64.7
Donepezil	—	—	—	—	0.02 ± 0.01	7.42 ± 0.39	371
AP2238	—	—	—	—	0.044 ± 0.006	48.9 ± 3.7	1111

[a] Human recombinant AChE and BuChE from human serum were used. IC_{50} values represent the concentration of inhibitor required to decrease enzyme activity by 50% and are the mean of two independent measurements, each performed in triplicate (SEM = standard error of the mean).

Table 2
Inhibitory activity on human AChE and BuChE, IC_{50} ratio of the studied compounds

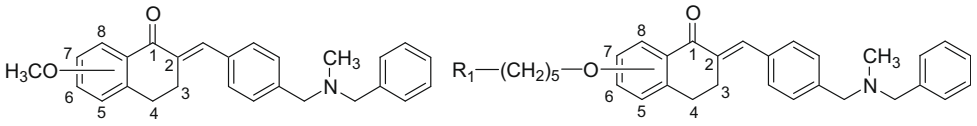

18-20 **21-22**

Compd	OCH_3 or chain position	R_1	IC_{50} hAChE (μM) ± SEM[a]	IC_{50} hBuChE (μM) ± SEM[a]	Ratio IC_{50} BuChE/AChE
18	6	—	0.11 ± 0.01	90.3 ± 3.8	820
19	7	—	5.38 ± 0.84	135 ± 32	25.1
20	6,7	—	0.18 ± 0.01	72.8 ± 5.0	404
21	6	NEt_2	0.056 ± 0.003	8.05 ± 0.50	144
22	6		0.052 ± 0.002	5.01 ± 0.19	96.3
Donepezil	—	—	0.02 ± 0.01	7.42 ± 0.39	371
AP2238	—	—	0.044 ± 0.006	48.9 ± 3.7	1111

[a] Human recombinant AChE and BuChE from human serum were used. IC_{50} values represent the concentration of inhibitor required to decrease enzyme activity by 50% and are the mean of two independent measurements, each performed in triplicate (SEM = standard error of the mean).

its interaction with the PAS. Again, position 5 of the indanone ring proved not to be optimal, independently of the chain's length (n = 2–4, compounds **6–8**), while the substitution in position 6 (compounds **9–11**, **14**, **16–17**) resulted in a general improvement of the activity, along with the elongation of the chain, the optimum being n = 5 (compound **14**). The trend was inverted when n = 6–7 (compounds **16–17**). We then changed the nature of the second amino moiety by replacing the diethylamino group with morpholine and piperidine. While the effect of morpholine was negligible (**12**), the introduction of piperidine with n = 4, (**13**) increased the activity by 5 times compared to the diethylamino derivative (**11**). Yet, when n = 5 no such increase in potency was noted for the piperidine substituent (**15**) with respect to the diethylamino (**14**). Concerning the tetralone series, replacing the methoxy substituent in position 6 by a pentyl chain (compound **21**) resulted in a remarkable increase in activity, comparable with that of the corresponding piperidine derivative (**22**). These two latter compounds proved to be the most active within the series and their potency against hAChE was in the same order of magnitude of the reference compounds. These derivatives also showed a good inhibition of hBuChE activity, with selectivity values lower than donepezil and AP2238. Several new lines of evidence suggest that BuChE might be a co-regulator of the activity of the neurotransmitter ACh, and that it might be important to inhibit this enzyme in the treatment of AD.[19,20] The marketed drug Rivastigmine also inhibits BuChE, providing dual AChE and BuChE inhibition.[21] It has been suggested

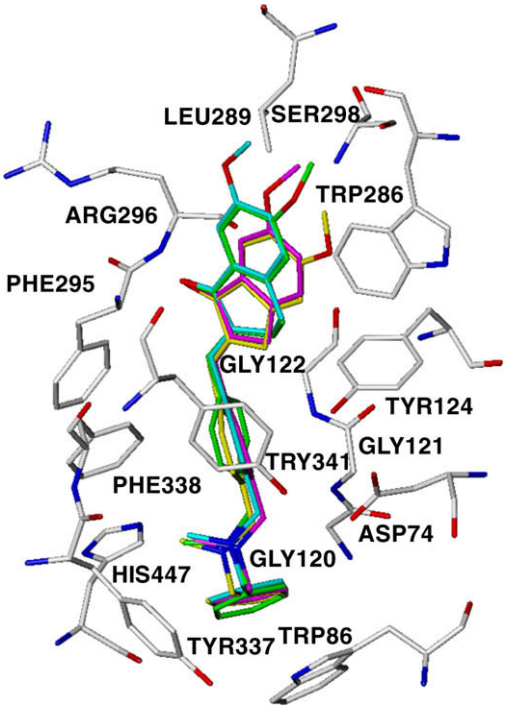

Figure 2. Docking of **2** (carbon atoms in yellow), **3** (carbon atoms in magenta), **18** (carbon atoms in green), and **19** (carbon atoms in cyan) into the gorge of the human AChE enzyme. All molecules are able to properly contact both sites of the enzyme, i.e. the catalytic pocket around Trp86 and the PAS in the region of Trp286. Further interactions could be also identified with the side chains of the residues of the mid-gorge[27–29] (Tyr124, Tyr337, and Tyr341, for a detailed description see the text). The interaction mode of the present inhibitors strictly resembles the binding of donepezil at the *Torpedo californica* AChE gorge (PDB code: 1eve[30]).

that dual inhibition may afford several advantages, including greater and broader symptomatic effects, particular behavioral benefits and the absence of AChE upregulation. These benefits are likely to increase with time, because, as AD progresses, AChE activity decreases by up to 45%, while BuChE activity increases by 40–90%. The gradual shift from AChE to BuChE in the enzyme responsible for degrading ACh during AD progression could be responsible for the inefficacy of AChE selective inhibitors. Consequently, there is a rationale for switching from a selective AChE inhibitor to an inhibitor of both AChE and BuChE.[21]

The in vitro determination of the inhibitory constant (61.1 ± 2.3 nM) of compound **22**, the most active derivative of these new series, confirmed the mixed type mechanism of action and, therefore, the possibility for **22** of contacting both the active and the peripheral binding sites of AChE. In fact, the pattern of the overlaid Lineweaver–Burk plots (Fig. 3) showed both increasing slopes and higher K_m at increasing inhibitor concentrations.

Some compounds, properly selected on the basis of their inhibitory potencies, were also tested for their ability to prevent AChE-induced Aβ aggregation. In particular, compounds **3**, **14–15** and **22** were screened at a single concentration and compared with reference compounds donepezil and AP2238. The limited selection of compounds to undergo AChE-induced Aβ aggregation assay is due to the high costs of the recombinant proteins involved in this assay. Considering that AChE inhibition and AChE-induced beta-amyloid aggregation do not represent independent phenomena, but both can be modulated by AChE PAS binding inhibitors, a rational selection was made on the basis of the lowest IC_{50} values obtained in Ellman's assay as well as of the dual binding mode of action. On the other hand, compound **3** represents an internal reference of the indanone series with regards to the role of the amino methylene chain at position 6. The obtained inhibitory activities, expressed as% inhibition, are reported in Table 3. Compound **3**, bearing a methoxy substituent in position 6, was not able to inhibit AChE-induced Aβ aggregation, whereas **14–15** and **22**, with a pentyl chain bearing a second amino moiety, showed some activity. In particular, **15** and **22**, piperidine derivatives, proved to be more active than the diethylamino derivative **14** (46.8% and 48.3% compared with 29.7%). In order to highlight the specific residues involved in the interaction, **14** and **15** underwent molecular modeling studies (Fig. 4). The molecules were found to contact both sites of the enzyme. However, the aliphatic chains of **14** and **15** can better contact Trp286 and partially protrude towards the bulk of the solvent. These features can be responsible for the inhibition of AChE-induced Aβ aggregation experimentally observed for **14** and **15**, but not for **3**. We can argue that the positive charge at the end of the aliphatic chains of **14** and **15** can be responsible for an electrostatic repulsion with the Aβ peptide, preventing its interaction with the PAS, which is fundamental for the chaperon-like effect of AChE towards Aβ fibril formation.

Finally, in the search for new multipotent compounds, the selected derivatives were evaluated against self-aggregation of $A\beta_{42}$ peptide, the most amyloidogenic form of amyloid produced in AD brains. Previously selected lead compounds (donepezil and AP2238) as well as **3** resulted completely ineffective in avoiding amyloid spontaneous aggregation (Table 3). On the other hand, **14**, **15**, **21** and **22**, when tested at 10 μM, showed a significant even if low inhibitory activity (26–28%).

5. Conclusions

We reported a new series of indanone hybrids bearing a pharmacophoric fragment of AP2238. This study was aimed at improving the activities of the reference compounds, donepezil and AP2238, and at broadening the range of activities of new derivatives as, due to the multifactorial nature of AD, molecules that

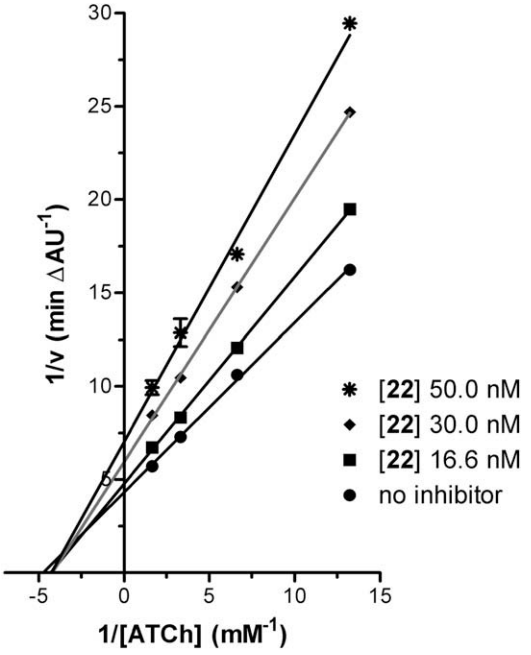

Figure 3. Steady-state inhibition by **22** of hydrolysis of acetylthiocholine (ATCh) by human recombinant AChE. Reciprocal plot of initial velocity (v) and substrate concentration at increasing inhibitor concentrations are reported. Reciprocal plot of initial velocity in the absence of inhibitor gave an estimate of k_{app} for ATCh of 170 ± 15 μM. Lines were derived from a weighted least-squares analysis of the data points.

Table 3
Inhibitory activity AChE-mediated Aβ aggregation and against β-amyloid (**1**–**42**) self-aggregation of the selected compounds

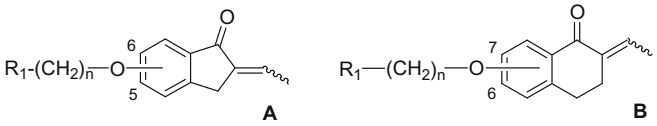

Compd	Structure	*n*	Position	R_1	Inhibition of AChE-induced $A\beta_{40}$ aggregation[a] ± SEM (%)	Inhibition of $A\beta_{42}$ self-aggregation[b] ± SEM (%)
3	A	—	6-OCH_3	—	<5	<5
14	A	5	6	NEt_2	29.7 ± 3.8	27.7 ± 3.6
15	A	5	6		46.8 ± 2.0	27.9 ± 4.0
21	B	5	6	NEt_2	42.9 ± 0.8	26.4 ± 1.1
22	B	5	6		48.3 ± 0.9	26.9 ± 3.4
Donepezil					22[c]	<5
AP2238					35	<5

[a] Determined at [inhibitor] = 100 μM, [$A\beta_{40}$] = 230 μM and [hAChE] = 2.3 μM.
[b] [$A\beta_{42}$] = 50 μM; [*I*] = 10 μM. Values are the mean of two independent measurements, each performed in duplicate. (SEM = standard error of the mean).
[c] Data obtained from Ref. 22.

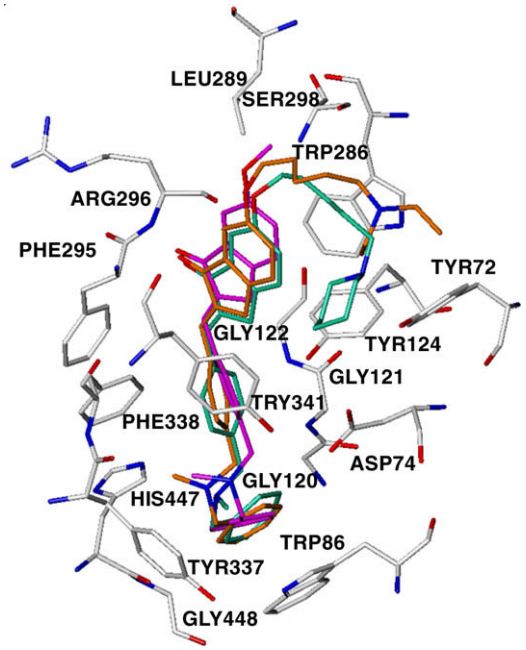

Figure 4. Docking of **14** (carbon atoms in orange), **15** (carbon atoms in light green), and **3** (carbon atoms in magenta) into the gorge of the human AChE enzyme. The molecules contact both sites of the enzyme. However, the aliphatic chain of **14** and **15** can better contact Trp286 and partially protrude towards the bulk of the solvent. The poses reported in the Figure are docking configurations representative of clusters statistically populated according to the Chaevenaut criterion, implemented in the AClAP 1.0 code.

modulate the activity of a single protein target are unable to significantly modify the progression of the disease. Derivatives **21** and **22** proved to be the most active within the series and their potency against AChE was in the same order of magnitude of the reference compounds. Compounds **15**, **21–22**, with a 5-carbon alkyl chain bearing an amino moiety at one end, better contacting the PAS, remarkably improved the inhibition of AChE-induced Aβ aggregation, with respect to the reference compounds. They also showed activity against self-aggregation of $A\beta_{42}$ peptide, while the reference compounds resulted completely ineffective. On the basis of the promising results obtained with the new compounds, **15**, **21** and **22** could represent new templates for further optimization studies.

6. Experimental section

6.1. Chemistry

6.1.1. General methods

All melting points were determined in open glass capillaries using a Büchi apparatus and are uncorrected. ^1H NMR and ^{13}C NMR spectra were recorded in $CDCl_3$ solution on a Varian Gemini 300 MHz spectrometer with Me_4Si as the internal standard. Chemical shifts are reported in parts per million (ppm) relative to tetramethylsilane (TMS), and multiplicities are given as s (singlet), d (doublet), t (triplet), m (multiplet) or br (broad). Mass spectra were recorded on a Waters ZQ 4000 apparatus operating in electrospray (ES) mode. Chromatographic separations were performed on silica gel columns (Kieselgel 40, 0.040–0.063 mm; Merck) by flash chromatography. The purity of the tested compounds was determined by HPLC analysis, performed on a Jasco LC 1500 PU-1587; the column used was a Phenomenex Luna C18(2) 5 μm × 4.60 mm × 150 mm; elution conditions: mobile phase CH_3CN/H_2O 50:50; the flow-rate was 0.8 mL/min and the injection volume was 5 μL; peaks were detected at 250 nm and results were >95% purity. Elemental analyses are indicated with element symbols, analytical results obtained for those elements were within 0.4% of the theoretical values. Compounds' names were obtained using AUTONOM, PC software for nomenclature in organic chemistry, Beilstein-Institute and Springer.

6.1.2. 4-Bromomethylbenzonitrile (23)

To a solution of 4-methylbenzonitrile (10.0 g, 0.088 mol) in CCl_4 (100 mL), NBS (15.6 g, 0.088 mol) was added in the presence of a catalytic amount of benzoyl peroxide. The mixture was refluxed for 5 h and hot filtered to remove the succinimide. The filtrate was evaporated under reduced pressure to give the crude product **23** (15.86 g, 92%) as yellow solid used for the next step without further purification.

6.1.3. 4-[(Benzylmethylamino)methyl]benzonitrile (24)

A solution of **23** (18.91 g, 0.096 mol) and *N*-benzylmetilamine (24.9 mL, 0.19 mol) in toluene (250 mL) was refluxed for 8 h. After cooling, the reaction mixture was washed with H_2O, dried (Na_2SO_4) and evaporated to dryness affording **24** (14.43 g, 64%). ^1H NMR δ 2.15 (s, 3H), 3.50 (s, 4H), 7.20–7.60 (m, 9H, Ar).

6.1.4. 4-[(Benzylethylamino)methyl]benzonitrile (25)

Using the previous procedure and starting from **23** (19 g, 0.097 mol) and *N*-benzylethylamine (28.5 mL, 0.194 mol), **25** (18 g, 74%) was obtained as a yellow oil. ^{1}H NMR δ 1.00 (t, 3H), 2.35–2.55 (m, 2H), 3.50 (s, 4H), 7.00–7.75 (m, 9H, Ar).

6.1.5. 4-[(Benzylmethylamino)methyl]benzaldehyde (26)

A mixture of **24** (6.85 g, 29 mmol) and Ni/Raney alloy (13.7 g) in 75% HCOOH (138 mL) was refluxed for 7 h, and then hot filtered. The residue was diluted with 100–150 mL of H_2O, basified by K_2CO_3 and extracted three times with CH_2Cl_2. The combined organic extracts were dried (Na_2SO_4), filtered and concentrated under reduced pressure to afford **26** (6.0 g, 87%) as yellow oil (purified by flash chromatography toluene/acetone 9:1 as eluent). ^{1}H NMR δ 2.20 (s, 3H), 3.50 (s, 4H), 7.20–7.80 (m, 9H, Ar), 10.00 (s, 1H).

6.1.6. 4-[(Benzylethylamino)methyl]benzaldehyde (27)

Using the previous procedure and starting from **25** (10 g, 0.097 mol), **27** (9.22 g, 78%) was obtained as yellow oil (purified by flash chromatography with toluene/acetone 4.8:0.2). ^{1}H NMR δ 1.00 (t, 3H), 2.35–2.55 (m, 2H), 3.50 (s, 4H), 7.00–7.75 (m, 9H, Ar), 9.90 (s, 1H).

6.1.7. 5-(2-Chloroethoxy)indan-1-one (28a)

A stirred mixture of 5-hydroxyindan-1-one (3.0 g, 0.020 mol), 1-bromo-2-chloroethane (10 mL, 0.040 mol) and K_2CO_3 (6 g) in acetone (250 mL) was refluxed for 24 h. The mixture was hot filtered and the solvent was removed. After adding petroleum ether, the residue was kept at −18 °C overnight, the white solid that formed was filtered off affording **28a** (3.83 g, 91%). Mp 81–82 °C. ^{1}H NMR δ 2.70 (t, 2H), 3.10 (t, 2H), 3.85 (t, 2H), 4.30 (t, 2H), 6.85–7.75 (m, 3H, Ar).

6.1.8. 5-(3-Chloropropoxy)indan-1-one (28b)

Using the previous procedure and starting from 5-hydroxyindan-1-one (3.0 g, 0.020 mol) and 1-bromo-3-chloropropane (10.1 mL, 0.040 mol), **28b** (3.69 g, 82%) was obtained as white solid. Mp 90–91 °C. ^{1}H NMR δ 2.20–2.40 (m, 2H), 2.70 (t, 2H), 3.05 (t, 2H), 3.75 (t, 2H), 4.20 (t, 2H), 6.85–7.70 (m, 3H, Ar).

6.1.9. 5-(4-Chlorobutoxy)indan-1-one (28c)

Using the previous procedure and starting from 5-hydroxyindan-1-one (4.0 g, 0.027 mol) and 1-bromo-4-chlorobutane (13.8 mL, 0.054 mol), **28c** (4.28 g, 67%) was obtained as white solid. Mp 52–53 °C. ^{1}H NMR δ 1.90–2.05 (m, 4H), 2.70 (t, 2H), 3.10 (t, 2H), 3.65 (t, 2H), 4.10 (t, 2H), 6.85–7.75 (m, 3H, Ar).

6.1.10. 6-(2-Chloroethoxy)indan-1-one (29a)

Using the previous procedure and starting from 6-hydroxyindan-1-one (1.5 g, di 0.010 mol) and 1-bromo-2-chloroethane (1.66 mL, 0.020 mol), **29a** (0.9 g, 43%) was obtained as white solid. Mp 59–60 °C. ^{1}H NMR δ 2.70 (t, 2H), 3.10 (t, 2H), 3.85 (t, 2H), 4.25 (t, 2H,), 7.10–7.40 (m, 3H, Ar).

6.1.11. 6-(3-Chloropropoxy)indan-1-one (29b)

Using the previous procedure and starting from 6-hydroxyindan-1-one (1.5 g, 0.010 mol) and 1-bromo-3-chloropropane (2 mL, 0.020 mol), **29b** (1.89 g, 84%) was obtained as white solid. Mp 50–51 °C. ^{1}H NMR δ 2.05–2.45 (m, 2H), 2.70 (t, 2H), 3.10 (t, 2H), 3.75 (t, 2H), 4.10 (t, 2H), 7.10–7.40 (m, 3H, Ar).

6.1.12. 6-(4-Chlorobutoxy)indan-1-one (29c)

Using the previous procedure and starting from 6-hydroxyindan-1-one (1.5 g, 0.010 mol) and 1-bromo-4-chlorobutane (2.31 mL, 0.020 mol), **29c** (2.17 g, 91%) was obtained as white solid. Mp 62–63 °C. ^{1}H NMR δ 1.80–2.05 (m, 4H), 2.70 (t, 2H), 3.05 (t, 2H), 3.60 (t, 2H), 4.00 (t, 2H), 7.10–7.40 (m, 3H, Ar).

6.1.13. 6-(5-Chloropentyloxy)indan-1-one (29d)

Using the previous procedure and starting from 6-hydroxyindan-1-one (1.2 g, 0.008 mol) and 1-bromo-5-chloropentane (2.13 mL, 0.016 mol), **29d** (1.69 g, 83%) was obtained as white solid. Mp 59–60 °C. ^{1}H NMR δ 1.50–1.95 (m, 6H), 2.70 (t, 2H), 3.05 (t, 2H), 3.60 (t, 2H), 4.00 (t, 2H), 7.10–7.40 (m, 3H, Ar).

6.1.14. 6-(6-Chlorohexyloxy)indan-1-one (29e)

Using the previous procedure and starting from 6-hydroxyindan-1-one (1.0 g, 6.7 mmol) and 1-bromo-6-chlorohexane (2.0 mL, 13.5 mmol), **29e** (1.26 g, 71%) was obtained as white solid. Mp 61–62 °C. ^{1}H NMR δ 1.35–1.55 (m, 6H), 1.70–1.90 (m, 2H), 2.70 (t, 2H), 3.05 (t, 2H), 3.50 (t, 2H), 4.00 (t, 2H), 7.10–7.40 (m, 3H, Ar).

6.1.15. 6-(7-Bromoheptyloxy)indan-1-one (29f)

Using the previous procedure and starting from 6-hydroxyindan-1-one (1.0 g, 6.7 mmol) and 1,7-dibromoheptane (2.76 mL, 3.4 mmol), **29f** (0.9 g, 41%) was obtained as yellow solid. Mp 36–37 °C. ^{1}H NMR δ 1.35–1.55 (m, 6H), 1.70–1.90 (m, 4H), 2.70 (t, 2H), 3.05 (t, 2H), 3.40 (t, 2H), 3.95 (t, 2H), 7.05–7.35 (m, 3H, Ar).

6.1.16. 6-(5-Chloropentyloxy)-3,4-dihydro-2*H*-naphthalen-1-one (30d)

Using the previous procedure and starting from 6-hydroxy-3,4-dihydro-2*H*-naphthalen-1-one (1.2 g, 7.4 mmol) and 1-bromo-5-chloropentane (1.95 mL, 14.8 mmol), **30d** (1.49 g, 76%) was obtained. Mp 25–26 °C. ^{1}H NMR δ 1.60–1.90 (m, 6H), 2.00–2.20 (m, 2H), 2.60 (t, 2H), 2.90 (t, 2H), 3.60 (t, 2H), 4.00 (t, 2H), 6.70–8.00 (m, 3H, Ar).

6.1.17. 2-{4-[(Benzylmethylamino)methyl]benzylidene}-5-(2-chloroethoxy)indan-1-one (31a)

To a solution of NaOH (0.58 g) in EtOH (72 mL), **28a** (1.5 g, 0.007 mol) was added and the reaction mixture was stirred for 1 h. Then, a solution of **26** (1.67 g, 0.007 mol) in a small amount of EtOH was added dropwise and the resulting mixture was stirred at room temperature overnight. The solid that formed was filtered off affording **31a** (1.30 g, 43%). Mp 100–101 °C. ^{1}H NMR δ 2.20 (s, 3H), 3.55 (s, 4H), 3.85 (t, 2H), 4.00 (s, 2H), 4.35 (t, 2H), 7.00–7.85 (m, 13H, Ar).

6.1.18. 2-{4-[(Benzylmethylamino)methyl]benzylidene}-5-(3-chloropropoxy)indan-1-one (31b)

Using the previous procedure and starting from **28b** (1.50 g, 6.7 mmol), **31b** (1.45 g, 49%) was obtained as white solid. Mp 111–113 °C. ^{1}H NMR δ 2.20 (s, 3H), 2.20–2.35 (m, 2H), 3.55 (s, 4H), 3.75 (t, 2H), 4.00 (s, 2H), 4.25 (t, 2H), 7.00–7.85 (m, 13H, Ar).

6.1.19. 2-{4-[(Benzylmethylamino)methyl]benzylidene}-5-(4-chlorobutoxy)indan-1-one (31c)

Using the previous procedure and starting from **28c** (1.50 g, 6.3 mmol), **31c** (1.32 g, 46%) was obtained as pale brown solid. Mp 113–114 °C. ^{1}H NMR δ 1.90–2.05 (m, 4H), 2.20 (s, 3H), 3.55 (s, 4H), 3.65 (t, 2H), 4.00 (s, 2H), 4.10 (t, 2H), 6.85–7.85 (m, 13H, Ar).

6.1.20. 2-{4-[(Benzylmethylamino)methyl]benzylidene}-6-(2-chloroethoxy)indan-1-one (32a)

Using the previous procedure and starting from **29a** (0.9 g, 4.3 mmol), **32a** (0.88 g, 48%) was obtained as pale brown solid. Mp 92–93 °C. ^{1}H NMR δ 2.20 (s, 3H), 3.50 (s, 4H), 3.85 (t, 2H), 4.00 (s, 2H), 4.30 (t, 2H), 7.20–7.70 (m, 13H, Ar).

6.1.21. 2-{4-[(Benzylmethylamino)methyl]benzylidene}-6-(3-chloropropoxy)indan-1-one (32b)

Using the previous procedure and starting from **29b** (1.21 g, 5.4 mmol), **32b** (1.06 g, 37%) was obtained as pale brown solid. Mp 120–121 °C d. ^{1}H NMR δ 1.80–2.05 (m, 2H), 2.20 (s, 3H), 3.25 (t, 2H), 3.55 (s, 4H), 3.60 (t, 2H), 3.90 (s, 2H), 4.05 (t, 2H), 7.10–7.60 (m, 13H, Ar).

6.1.22. 2-{4-[(Benzylmethylamino)methyl]benzylidene}-6-(4-chlorobutoxy)indan-1-one (32c)

Using the previous procedure and starting from **29c** (1.44 g, 6 mmol), **32c** (1.66 g, 60%) was obtained as pale brown solid. Mp 90–91 °C. ^{1}H NMR δ 1.90–2.10 (m, 4H), 2.20 (s, 3H), 3.55 (s, 4H), 3.60 (t, 2H), 4.00 (t, 2H), 4.10 (t, 2H), 7.10–7.65 (m, 13H, Ar).

6.1.23. 2-{4-[(Benzylmethylamino)methyl]benzylidene}-6-(5-chloropentoxy)indan-1-one (32d)

Using the previous procedure and starting from **29d** (1.69 g, 6.7 mmol), **32d** (1.72 g, 55%) was obtained as solid. Mp 71–72 °C. ^{1}H NMR δ 1.55–1.95 (m, 6H), 2.20 (s, 3H), 3.55 (s, 4H), 3.60 (t, 2H), 3.95 (t, 2H), 4.10 (t, 2H), 7.20–7.75 (m, 13H, Ar).

6.1.24. 2-{4-[(Benzylmethylamino)methyl]benzylidene}-6-(6-chlorohexiloxy)indan-1-one (32e)

Using the previous procedure and starting from **29e** (1.00 g, 3.8 mmol), **32e** (1.30 g, 70%) was obtained as white solid. Mp 94–95 °C. ^{1}H NMR δ 1.45–1.65 (m, 8H), 2.20 (s, 3H), 3.55 (s, 4H), 3.70 (t, 2H), 4.00 (t, 2H), 4.10 (t, 2H), 7.10–7.65 (m, 13H, Ar).

6.1.25. 2-{4-[(Benzylmethylamino)methyl]benzylidene}-6-(7-bromoheptyloxy)indan-1-one (32f)

Using the previous procedure and starting from **29f** (1.30 g, 4 mmol), **32f** (1.20 g, 55%) was obtained as white solid. Mp 90–91 °C. ^{1}H NMR δ 1.35–1.60 (m, 6H), 1.75–1.95 (m, 4H), 2.20 (s, 3H), 3.40 (t, 2H), 3.55 (s, 4H), 3.80–4.10 (m, 4H), 7.20–7.65 (m, 13H, Ar).

6.1.26. 2-{4-[(Benzylmethylamino)methyl]benzylidene}-6-(5-chloropentyloxy)-3,4-dihydro-*2H*-naphthalen-1-one (33d)

Using the previous procedure and starting from **30d** (1.50 g, 5.6 mmol), **33d** (0.42 g, 15%) was obtained as yellow oil (purified by flash chromatography with toluene/acetone 4.8:0.2). ^{1}H NMR δ 1.55–1.70 (m, 2H), 1.75–1.90 (m, 4H), 2.20 (s, 3H), 2.90 (t, 2H), 3.10 (t, 2H), 3.50–3.55 (m, 6H), 4.00 (t, 2H), 6.65–8.10 (m, 13H, Ar).

6.1.27. 2-{4-[(Benzylmethylamino)methyl]benzylidene}-5-(2-iodoethoxy)indan-1-one (34a)

A mixture of **31a** (1.20 g, 2.8 mmol) and NaI (0.42 g, 2.8 mmol) in methylethylketone (20 mL) was refluxed for 4 h. After cooling, the separated solid was collected by filtration, affording **34a** (0.9 g, 61%). Mp 94–96 °C. ^{1}H NMR δ 2.20 (s, 3H), 3.55 (s, 4H), 3.85 (t, 2H), 4.00 (s, 2H), 4.35 (t, 2H), 7.00–7.85 (m, 13H, Ar).

6.1.28. 2-{4-[(Benzylmethylamino)methyl]benzylidene}-5-(3-iodopropoxy)indan-1-one (34b)

Using the previous procedure and starting from **31b** (1.60 g, 3.6 mmol), **34b** (2.44 g, 72%) was obtained as yellow solid. Mp 112–114 °C. ^{1}H NMR δ 2.20 (s, 3H), 2.25–2.40 (m, 2H), 3.40 (t, 2H), 3.55 (s, 4H), 4.00 (s, 2H), 4.25 (t, 2H), 7.00–7.85 (m, 13H, Ar).

6.1.29. 2-{4-[(Benzylmethylamino)methyl]benzylidene}-5-(4-iodobutoxy)indan-1-one (34c)

Using the previous procedure and starting from **31c** (1.20 g, 2.6 mmol), **34c** (1.10 g, 77%) was obtained as solid. Mp 87–88 °C. ^{1}H NMR δ 1.90–2.10 (m, 4H), 2.20 (s, 3H), 3.30 (t, 2H), 3.55 (s, 4H), 4.00 (s, 2H), 4.10 (t, 2H), 6.90–7.85 (m, 13H, Ar).

6.1.30. 2-{4-[(Benzylmethylamino)methyl]benzylidene}-6-(2-iodoethoxy)indan-1-one (35a)

Using the previous procedure and starting from **32a** (0.40 g, 0.93 mmol), **35a** (0.31 g, 64%) was obtained as yellow oil. ^{1}H NMR δ 2.20 (s, 3H), 3.55 (s, 4H), 3.80 (t, 2H), 3.95 (s, 2H), 4.30 (t, 2H), 7.20–7.60 (m, 13H, Ar).

6.1.31. 2-{4-[(Benzylmethylamino)methyl]benzylidene}-6-(3-iodopropoxy)indan-1-one (35b)

Using the previous procedure and starting from **32b** (0.80 g, 1.8 mmol), **35b** (1.22 g, 72%) was obtained as yellow solid. Mp 110–112 °C. ^{1}H NMR δ 2.20 (s, 3H), 2.25–2.40 (m, 2H), 3.40 (t, 2H), 3.55 (s, 4H), 4.00 (s, 2H), 4.25 (t, 2H), 7.00–7.85 (m, 13H, Ar).

6.1.32. 2-{4-[(Benzylmethylamino)methyl]benzylidene}-6-(4-iodobutoxy)indan-1-one (35c)

Using the previous procedure and starting from **32c** (0.80 g, 1.8 mmol), **35c** (0.89 g, 95%) was obtained as yellow oil. ^{1}H NMR δ 1.80–2.05 (m, 4H), 2.20 (s, 3H), 3.25 (t, 2H), 3.55 (s, 4H), 3.60 (t, 2H), 3.90 (s, 2H), 4.05 (t, 2H), 7.10–7.60 (m, 13H, Ar).

6.1.33. 2-{4-[(Benzylmethylamino)methyl]benzylidene}-6-(5-iodopentyloxy)indan-1-one (35d)

Using the previous procedure and starting from **32d** (0.30 g, 0.63 mmol), **35d** (0.22 g, 69%) was obtained as yellow oil. ^{1}H NMR δ 1.40–1.90 (m, 6H), 2.20 (s, 3H), 3.20 (t, 2H), 3.55 (s, 4H), 3.60 (t, 2H), 3.80–4.10 (m, 4H), 7.00–7.60 (m, 13H, Ar).

6.1.34. 2-{4-[(Benzylmethylamino)methyl]benzylidene}-6-(6-iodohexiloxy)indan-1-one (35e)

Using the previous procedure and starting from **32e** (1.30 g, 2.7 mmol), **35e** (1.50 g, 97%) was obtained as yellow solid. Mp 90–91 °C. ^{1}H NMR δ 1.40–1.60 (m, 4H), 1.70–1.90 (m, 4H), 2.20 (s, 3H), 3.20 (t, 2H), 3.55 (s, 4H), 3.90–4.10 (m, 4H), 7.10–7.70 (m, 13H, Ar).

6.1.35. 2-{4-[(Benzylmethylamino)methyl]benzylidene}-6-(5-iodopentyloxy)-3,4-dihydro-*2H*-naphthalen-1-one (36d)

Using the previous procedure and starting from **33d** (0.39 g, 0.8 mmol), **36d** (0.32 g, 69%) was obtained as yellow oil. ^{1}H NMR δ 1.50–2.00 (m, 6H), 2.20 (s, 3H), 2.90 (t, 2H), 3.10 (t, 2H), 3.20 (t, 2H), 3.55 (s, 4H), 4.00 (t, 2H), 6.65–8.10 (m, 13H, Ar).

6.1.36. 2-{4-[(Benzylmethylamino)methyl]benzylidene}-5,6-dimethoxyindan-1-one (1)

To a solution of pellets NaOH (0.21 g) in EtOH (30 mL), 5,6-dimethoxyindan-1-one (0.5 g, 2.6 mmol) was added and the reaction mixture was stirred for 1 h. A solution of **26** (0.62 g, 2.6 mmol) in a small amount of EtOH was added dropwise and the resulting mixture was stirred at room temperature overnight. The solid that formed was filtered off affording **1** (0.87 g, 81%) as yellow solid. Mp 147–148 °C (ligroine), HCl mp 249–250 °C (EtOH/Et_2O). ^{1}H NMR δ 2.20 (s, 3H), 3.55 (s, 4H), 3.95–4.10 (m, 8H), 7.00–7.75 (m, 12H, Ar). ^{13}C NMR δ 31.83, 42.31, 56.12, 56.64, 61.42, 61.91, 105.75, 118.66, 118.82, 123.84, 126.87, 127.03, 128.26, 133.74, 134.13, 135.09, 139.29, 141.46, 150.95, 153.37, 145.23, 197.99. MS (ES) *m/z*: 414 ($M+H^+$). Anal. $C_{27}H_{27}NO_3$ (C, H, N).

6.1.37. 2-{4-[(Benzylmethylamino)methyl]benzylidene}-5-methoxyindan-1-one (2)

Using the previous procedure and starting from 5-methoxyindan-1-one (1.00 g, 6.0 mmol) and **26** (1.47 g, 6.0 mmol), **2** (0.84 g, 31%) was obtained as white solid. Mp 130–131 °C (toluene). ^{1}H NMR δ 2.20 (s, 3H), 3.55 (s, 4H), 3.90 (s, 3H), 4.00 (s, 2H), 7.00–7.90 (m, 13H, Ar). ^{13}C NMR δ 31.83, 42.31, 55.63, 61.42, 61.91, 105.75, 118.72, 115.08, 123.84, 126.87, 127.03, 128.26, 129.35,

130.74, 134.13, 135.09, 139.29, 141.46, 150.95, 167.56, 197.99. MS (ES) *m/z*: 384 ($M+H^+$). Anal. $C_{26}H_{25}NO_2$ (C, H, N).

6.1.38. 2-{4-[(Benzylmethylamino)methyl]benzylidene}-6-methoxyindan-1-one (3)

Using the previous procedure and starting from 6-methoxyindan-1-one (1.47 g, 9.0 mmol) and **26** (2.17 g, 9.0 mmol), **3** (0.30 g, 10%, purified by flash chromatography with toluene/acetone 4.5:0.5) was obtained as white solid. Mp 119–120 °C. ^1H NMR δ 2.20 (s, 3H), 3.55 (s, 4H), 3.80 (s, 3H), 3.90 (s, 2H), 7.10–7.65 (m, 13H, Ar). ^{13}C NMR δ 31.83, 42.31, 55.63, 61.42, 61.91, 105.75, 123.84, 126.87, 127.03, 128.26, 129.35, 130.72, 133.74, 134.13, 135.09, 139.04, 139.29, 141.46, 142.42, 150.95, 159.57, 197.99. MS (ES) *m/z*: 384 ($M+H^+$). Anal. $C_{26}H_{25}NO_2$ (C, H, N).

6.1.39. 2-{4-[(Benzylethylamino)methyl]benzylidene}-6-methoxyindan-1-one (4)

Using the previous procedure and starting from 6-methoxyindan-1-one (0.50 g, 3.1 mmol) and **27** (0.78 g, 3.1 mmol), **4** was obtained as oil, purified by flash chromatography with toluene/acetone 4.7:0.3. The purified compound was converted into the hydrochloride salt affording **4**·HCl (0.63 g, 20%): mp 218–219 °C ($EtOH/Et_2O$). ^1H NMR δ 1.05 (t, 3H), 2.50–2.55 (m, 2H), 3.55 (s, 4H), 3.85 (s, 3H), 3.95 (s, 2H), 7.10–7.65 (m, 13H, Ar). ^{13}C NMR δ 10.78, 31.83, 48.93, 55.63, 59.02, 59.48, 105.75, 126.01, 126.87, 127.03, 128.26, 129.35, 130.72, 133.74, 134.13, 135.09, 139.29, 141.46, 141.84, 150.95, 197.99. MS (ES) *m/z*: 398 ($M+H^+$). Anal. $C_{27}H_{27}NO_2$ (C, H, N).

6.1.40. 2-{4-[(Benzylmethylamino)methyl]benzylidene}indan-1-one (5)

Using the previous procedure and starting from indan-1-one (0.28 g, 2.0 mmol) and **26** (0.50 g, 2.0 mmol), **5** was obtained as oil, purified by flash chromatography with toluene/acetone 4.8:0.2. The purified compound was converted in the hydrochloride salt affording **5**·HCl (0.10 g, 14%): mp 246–247 °C ($EtOH/Et_2O$).^1H NMR δ 2.20 (s, 3H), 3.55 (s, 4H), 4.00 (s, 2H), 7.10–7.90 (m, 14H, Ar). ^{13}C NMR δ 31.83, 42.31, 61.42, 61.91, 105.75, 123.84, 126.87, 127.03, 128.26, 129.35, 130.72, 133.74, 134.13, 135.09, 139.04, 139.29, 141.46, 142.42, 150.95, 159.57, 197.99. MS (ES) *m/z*: 354 ($M+H^+$). Anal. $C_{25}H_{23}NO$ (C, H, N).

6.1.41. 2-{4-[(Benzylmethylamino)methyl]benzylidene}-6-methoxy-3,4-dihydro-*2H*-naphthalen-1-one (18)

Using the previous procedure and starting from 6-methoxy-3,4-dihydro-*2H*-naphthalen-1-one (1.60 g, 9 mmol) and **26** (2.17 g, 9 mmol), **18** was obtained and purified by flash chromatography with toluene/acetone 4.7:0.3. The purified compound was obtained as white solid (0.50 g, 14%) mp 91–93 °C. ^1H NMR δ 2.20 (s, 3H), 2.85 (t, 2H), 3.10 (t, 2H), 3.55 (s, 4H), 3.85 (s, 3H), 6.70–8.10 (m, 13H, Ar). ^{13}C NMR δ 27.26, 29.28, 42.27, 55.43, 61.47, 61.88, 112.24, 113.29, 127.03, 127.10, 128.26, 128.91, 129.84, 130.74, 135.23, 135.95, 145.69, 163.53, 186.78. MS (ES) *m/z*: 398 ($M+H^+$). Anal. $C_{27}H_{27}NO_2$ (C, H, N).

6.1.42. 2-{4-[(Benzylmethylamino)methyl]benzylidene}-7-methoxy-3,4-dihydro-*2H*-naphthalen-1-one (19)

Using the previous procedure and starting from 7-methoxy-3,4-dihydro-*2H*-naphthalen-1-one (0.50 g, 2.8 mmol) and **26** (0.68 g, 2.8 mmol), **19** was obtained as oil and purified by flash chromatography with toluene/acetone 4.9:0.1. The purified compound was converted in the hydrochloride salt affording **20**·HCl (0.10 g, 13%): mp 220–221 °C ($EtOH/Et_2O$). ^1H NMR δ 2.20 (s, 3H), 2.85 (t, 2H), 3.10 (t, 2H), 3.55 (s, 4H), 3.85 (s, 3H), 7.00–7.85 (m, 13H, Ar). ^{13}C NMR δ 27.26, 29.28, 42.27, 55.43, 61.47, 61.88, 113.29, 114.24, 127.03, 127.10, 128.26, 128.91, 129.84, 130.74, 135.23, 135.95, 145.69, 157.57, 186.78. MS (ES) *m/z*: 398 ($M+H^+$). Anal. $C_{27}H_{27}NO_2$ (C, H, N).

6.1.43. 2-{4-[(Benzylmethylamino)methyl]benzylidene}-6,7-dimethoxy-3,4-dihydro-*2H*-naphthalen-1-one (20)

Using the previous procedure and starting from 6,7-methoxy-3,4-dihydro-*2H*-naphthalen-1-one (0.62 g, 3 mmol) and **26** (1.15 g, 4.8 mmol), **20** was obtained as yellow oil and purified by flash chromatography with toluene/acetone 96:4. ^1H NMR δ 2.20 (s, 3H), 2.90 (t, 2H), 3.10 (t, 2H), 3.55 (s, 4H), 3.85 (s, 6H), 6.70–8.10 (m, 12H, Ar). ^{13}C NMR δ 27.26, 29.28, 42.27, 55.43, 55.84, 61.47, 61.88, 113.29, 127.03, 127.10, 128.26, 128.91, 129.84, 130.74, 135.23, 135.95, 145.69, 147.34, 155.58, 186.78. MS (ES) *m/z*: 428 ($M+H^+$). Anal. $C_{28}H_{29}NO_2$ (C, H, N)

6.1.44. 2-{4-[(Benzylmethylamino)methyl]benzylidene}-5-(2-diethylaminoethoxy)indan-1-one (6)

A solution of **34a** (0.35 g, 0.67 mmol) and diethylamine (0.21 mL, 2 mmol) in toluene (50 mL) was refluxed for 20 h. The mixture was washed with water (3 × 25 mL) and the organic layer was dried over Na_2SO_4. The solvent was removed under reduced pressure and the residue was purified by flash chromatography (toluene/acetone 3:2), affording **6** as a yellowish solid (0.05 g, 16%). ^1H NMR δ 1.00 (t, 6H), 2.20 (s, 3H), 2.50–2.65 (m, 6H), 3.55 (s, 4H), 3.95 (s, 2H), 4.10 (t, 2H), 6.90–7.80 (m, 13H, Ar). ^{13}C NMR δ 9.82, 10.74, 31.83, 42.33, 46.66, 52.27, 61.42, 61.92, 66.13, 106.47, 124.16, 127.00, 128.24, 128.84, 129.33, 130.70, 133.70, 134.10, 135.09, 139.09, 141.52, 142.29, 158.95, 197.97. MS (ES) *m/z*: 469 ($M+H^+$). Anal. $C_{31}H_{36}N_2O_2$ (C, H, N).

6.1.45. 2-{4-[(Benzylmethylamino)methyl]benzylidene}-5-(3-diethylaminopropoxy)indan-1-one (7)

Using the previous procedure and starting from **34b** (0.40 g, 0.75 mmol), **7** (purified by flash chromatography with toluene/acetone 3:2) was obtained as yellow solid (0.24 g, 66%), mp 65–67 °C. ^1H NMR δ 1.00 (t, 6H), 1.85–2.00 (m, 2H), 2.20 (s, 3H), 2.55–2.65 (m, 6H), 3.55 (s, 4H), 3.95 (s, 2H), 4.10 (t, 2H), 6.90–7.80 (m, 13H, Ar). ^{13}C NMR δ 9.82, 10.74, 29.73, 31.81, 42.33, 46.66, 52.27, 61.42, 61.92, 66.13, 106.47, 124.16, 127.00, 128.24, 128.84, 129.33, 130.70, 133.70, 134.10, 135.09, 139.09, 141.52, 142.29, 158.95, 197.97. MS (ES) *m/z*: 483 ($M+H^+$). Anal. $C_{32}H_{38}N_2O_2$ (C, H, N).

6.1.46. 2-{4-[(Benzylmethylamino)methyl]benzylidene}-5-(4-diethylaminobutoxy)indan-1-one (8)

Using the previous procedure and starting from **34c** (0.10 g, 0.75 mmol), **8** (purified by flash chromatography with toluene/acetone 3:2) was obtained as yellow oil (0.03 g, 33%). ^1H NMR δ 1.00 (t, 6H), 1.60–1.90 (m, 4H), 2.20 (s, 3H), 2.40–2.55 (m, 6H), 3.55 (s, 4H), 4.00 (s, 2H), 4.10 (t, 2H), 6.90–7.80 (m, 13H, Ar). ^{13}C NMR δ 9.82, 10.74, 25.70, 28.93, 31.81, 42.33, 46.66, 50.07, 61.42, 61.92, 67.85, 106.47, 124.16, 127.00, 128.24, 128.84, 129.33, 130.70, 133.70, 134.10, 135.09, 139.09, 141.52, 142.29, 158.95, 197.97. MS (ES) *m/z*: 497 ($M+H^+$). Anal. $C_{33}H_{40}N_2O_2$ (C, H, N).

6.1.47. 2-{4-[(Benzylmethylamino)methyl]benzylidene}-6-(2-diethylaminoethoxy)indan-1-one (9)

Using the previous procedure and starting from **35a** (0.31 g, 0.6 mmol), **9** (purified by flash chromatography with toluene/acetone 4.5:0.5) was obtained as orange solid (0.06 g, 21%), mp 58–59 °C. ^1H NMR δ 1.00 (t, 6H), 2.20 (s, 3H), 2.50–2.65 (m, 4H), 2.95 (t, 2H), 3.55 (s, 4H), 4.00 (s, 2H), 4.15 (t, 2H), 7.10–7.70 (m, 13H, Ar). ^{13}C NMR δ 9.82, 10.74, 31.83, 42.33, 46.66, 52.27, 61.42, 61.92, 66.13, 106.47, 124.16, 127.00, 128.24, 128.84, 129.33, 130.70, 133.70, 134.10, 135.09, 139.09, 141.52, 142.29, 158.95, 197.97. MS (ES) *m/z*: 469 ($M+H^+$). Anal. $C_{31}H_{36}N_2O_2$ (C, H, N).

6.1.48. 2-{4-[(Benzylmethylamino)methyl]benzylidene}-6-(3-diethylaminopropoxy)indan-1-one (10)

Using the previous procedure and starting from **35b** (0.50 g, 0.9 mmol), **10** (purified by flash chromatography with toluene/acetone 90:10) was obtained as yellow solid (0.16 g, 37%), mp 80–81 °C. ^{1}H NMR δ 1.00 (t, 6H), 1.90–2.05 (m, 2H), 2.20 (s, 3H), 2.50–2.65 (m, 6H), 3.55 (s, 4H), 4.00 (s, 2H), 4.10 (t, 2H), 7.10–7.70 (m, 13H, Ar). ^{13}C NMR δ 9.82, 10.74, 29.73, 31.81, 42.33, 46.66, 52.27, 61.42, 61.92, 66.13, 106.47, 124.16, 127.00, 128.24, 128.84, 129.33, 130.70, 133.70, 134.10, 135.09, 139.09, 141.52, 142.29, 158.95, 197.97. MS (ES) *m/z*: 483 (M+H$^+$). Anal. $C_{32}H_{38}N_2O_2$ (C, H, N).

6.1.49. 2-{4-[(Benzylmethylamino)methyl]benzylidene}-6-(4-diethylaminobutoxy)indan-1-one (11)

Using the previous procedure and starting from **35c** (0.89 g, 1.6 mmol), **11** (purified by flash chromatography with toluene/acetone 4:1) was obtained as orange oil (0.09 g, 11%). ^{1}H NMR δ 1.00 (t, 6H), 1.55–1.70 (m, 2H), 1.75–1.85 (m, 2H), 2.20 (s, 3H), 2.45–2.65 (m, 6H), 3.55 (s, 4H), 4.00 (s, 2H), 4.05 (t, 2H), 7.10–7.70 (m, 13H, Ar). ^{13}C NMR δ 9.82, 10.74, 25.70, 28.93, 31.81, 42.33, 46.66, 50.07, 61.42, 61.92, 67.85, 106.47, 124.16, 127.00, 128.24, 128.84, 129.33, 130.70, 133.70, 134.10, 135.09, 139.09, 141.52, 142.29, 158.95, 197.97. MS (ES) *m/z*: 497 (M+H$^+$). Anal. $C_{33}H_{40}N_2O_2$ (C, H, N).

6.1.50. 2-{4-[(Benzylmethylamino)methyl]benzylidene}-6-(4-morpholin-4-yl-butoxy)indan-1-one (12)

Using the previous procedure and starting from **35c** (0.25 g, 0.45 mmol) and morpholine (0.08 mL, 0.91 mmol), **12** (purified by flash chromatography with toluene/acetone 4:1) was obtained as yellow solid (0.08 g, 35%), mp 93–94 °C. ^{1}H NMR δ 1.60–1.70 (m, 2H), 1.75–1.90 (m, 2H), 2.20 (s, 3H), 2.35–2.50 (m, 6H), 3.55 (s, 4H), 3.70 (t, 4H), 3.95 (s, 2H), 4.05 (t, 2H), 7.10–7.65 (m, 13H, Ar). ^{13}C NMR δ 25.89, 27.32, 31.81, 42.33, 54.61, 61.45, 61.95, 63.36, 68.20, 106.46, 124.22, 126.82, 126.99, 128.24, 128.84, 129.31, 130.69, 133.63, 134.14, 135.14, 139.13, 139.24, 141.50, 142.23, 159.01, 197.96. MS (ES) *m/z*: 511 (M+H$^+$). Anal. $C_{33}H_{38}N_2O_3$ (C, H, N).

6.1.51. 2-{4-[(Benzylmethylamino)methyl]benzylidene}-6-(4-piperidin-1-yl-butoxy)indan-1-one (13)

Using the previous procedure and starting from **35c** (0.25 g, 0.45 mmol) and piperidine (0.09 mL, 0.91 mmol), **13** (purified by flash chromatography with toluene/acetone 4:1) was obtained as yellow solid (0.08 g, 35%), mp 76–77 °C. ^{1}H NMR δ 1.30–1.90 (m, 10H), 2.20 (s, 3H), 2.25–2.45 (m, 6H), 3.55 (s, 4H), 3.95 (s, 2H), 4.05 (t, 2H), 7.10–7.70 (m, 13H, Ar). ^{13}C NMR δ 23.47, 24.47, 25.99, 27.31, 31.81, 42.33, 54.61, 59.04, 61.45, 61.95, 68.20, 106.46, 124.22, 126.82, 126.99, 128.24, 128.84, 129.31, 130.69, 133.63, 134.14, 135.14, 139.13, 139.24, 141.50, 142.23, 159.01, 197.96. MS (ES) *m/z*: 509 (M+H$^+$). Anal. $C_{34}H_{40}N_2O_2$ (C, H, N).

6.1.52. 2-{4-[(Benzylmethylamino)methyl]benzylidene}-6-(5-diethylaminopentyloxy)indan-1-one (14)

Using the previous procedure and starting from **35d** (0.30 g, 0.53 mmol), **14** (purified by flash chromatography with toluene/acetone 4:1) was obtained as yellow oil (0.03 g, 11%). ^{1}H NMR δ 1.00 (t, 6H), 1.40–1.90 (m, 6H), 2.20 (s, 3H), 2.40–2.60 (m, 6H), 3.55 (s, 4H), 3.95–4.05 (m, 4H), 7.10–7.65 (m, 13H, Ar). ^{13}C NMR δ 9.82, 10.74, 24.01, 25.70, 28.93, 31.81, 42.33, 46.66, 52.27, 61.42, 61.92, 68.13, 106.47, 124.16, 127.00, 128.24, 128.84, 129.33, 130.70, 133.70, 134.10, 135.09, 139.09, 141.52, 142.29, 158.95, 197.97. MS (ES) *m/z*: 511 (M+H$^+$). Anal. $C_{34}H_{42}N_2O_2$ (C, H, N).

6.1.53. 2-{4-[(Benzylmethylamino)methyl]benzylidene}-6-(5-piperidin-1-yl-pentyloxy)indan-1-one (15)

Using the previous procedure and starting from **35d** (0.25 g, 0.44 mmol) and piperidine (0.1 mL, 0.88 mmol), **15** (purified by flash chromatography with toluene/acetone 4:1) was obtained as yellow oil (0.08 g, 38%). ^{1}H NMR δ 1.30–1.65 (m, 8H), 1.75–2.00 (m, 4H), 2.20 (s, 3H), 2.25–2.45 (m, 6H), 3.75 (s, 4H), 3.95 (s, 2H), 4.05 (t, 2H), 7.10–7.70 (m, 13H, Ar). ^{13}C NMR δ 23.47, 24.47, 25.99, 27.31, 27.33, 31.81, 42.33, 54.61, 59.04, 61.45, 61.95, 68.02, 106.46, 124.22, 126.82, 126.99, 128.24, 128.84, 129.31, 130.69, 133.63, 134.14, 135.14, 139.13, 139.24, 141.50, 142.23, 159.01, 197.96. MS (ES) *m/z*: 523 (M+H$^+$). Anal. $C_{35}H_{42}N_2O_2$ (C, H, N).

6.1.54. 2-{4-[(Benzylmethylamino)methyl]benzylidene}-6-(6-diethylaminohexyloxy)indan-1-one (16)

Using the previous procedure and starting from **35e** (0.30 g, 0.5 mmol), **16** (purified by flash chromatography with toluene/acetone 4:1) was obtained as yellow solid (0.10 g, 38%), mp 63–64 °C. ^{1}H NMR δ 1.00 (t, 6H), 1.40–1.90 (m, 8H), 2.20 (s, 3H), 2.40–2.60 (m, 6H), 3.55 (s, 4H), 3.95–4.05 (m, 4H), 7.10–7.75 (m, 13H, Ar). ^{13}C NMR δ 9.82, 10.74, 24.01, 25.70, 28.93, 29.26, 31.81, 42.33, 46.66, 52.26, 61.42, 61.92, 68.14, 106.47, 124.16, 127.00, 128.24, 128.84, 129.33, 130.70, 133.70, 134.10, 135.09, 139.09, 141.52, 142.29, 158.95, 197.97. MS (ES) *m/z*: 525 (M+H$^+$). Anal. $C_{35}H_{44}N_2O_2$ (C, H, N).

6.1.55. 2-{4-[(Benzylmethylamino)methyl]benzylidene}-6-(7-diethylaminoheptyloxy)indan-1-one (17)

Using the previous procedure and starting from **32f** (0.30 g, 0.55 mmol), **17** (purified by flash chromatography with toluene/acetone 4:1) was obtained as yellow solid (0.07 g, 24%), mp 72 °C. ^{1}H NMR δ 1.00 (t, 6H), 1.20–1.60 (m, 8H), 1.70–1.90 (m, 2H), 2.20 (s, 3H), 2.35–2.60 (m, 6H), 3.55 (s, 4H), 3.90–4.10 (m, 4H), 7.10–7.65 (m, 13H, Ar). ^{13}C NMR δ 9.82, 10.74, 25.01, 25.70, 28.93, 29.26, 29.82, 31.81, 42.33, 46.66, 52.28, 61.42, 61.92, 68.14, 106.47, 124.16, 127.00, 128.24, 128.84, 129.33, 130.70, 133.70, 134.10, 135.09, 139.09, 141.52, 142.29, 158.95, 197.97. MS (ES) *m/z*: 539 (M+H$^+$). Anal. $C_{36}H_{46}N_2O_2$ (C, H, N).

6.1.56. 2-{4-[(Benzylmethylamino)methyl]benzylidene}-6-(5-diethylaminopentyloxy)-3,4-dihydro-*2H*-naphthalen-1-one (21)

Using the previous procedure and starting from **36d** (0.32 g, 0.55 mmol), **21** (purified by flash chromatography with toluene/acetone 4:1) was obtained as yellow oil (0.14 g, 49%). ^{1}H NMR δ 1.00 (t, 6H), 1.40–1.60 (m, 4H), 1.75–1.85 (m, 2H), 2.20 (s, 3H), 2.40 (t, 2H), 2.40–2.55 (m, 4H), 2.90 (t, 2H), 3.10 (t, 2H), 3.55 (s, 4H), 4.00 (t, 2H), 6.70–8.10 (m, 13H, Ar). ^{13}C NMR δ 9.82, 10.74, 24.01, 25.70, 28.93, 29.28, 27.25, 42.33, 46.66, 52.27, 61.42, 61.92, 68.13, 124.16, 127.00, 128.24, 128.84, 129.33, 130.70, 133.70, 134.10, 135.09, 139.09, 141.52, 142.29, 162.45, 187.97. MS (ES) *m/z*: 525 (M+H$^+$). Anal. $C_{35}H_{44}N_2O_2$ (C, H, N).

6.1.57. 2-{4-[(Benzylmethylamino)methyl]benzylidene}-6-(5-piperidin-1-yl-pentyloxy)-3,4-dihydro-*2H*-naphthalen-1-one (22)

Using the previous procedure and starting from **36d** (0.2 g, 0.35 mmol), **23** (purified by flash chromatography with toluene/acetone 4:1) was obtained as yellow oil (0.14 g, 77%). ^{1}H NMR δ 1.25–1.65 (m, 8H), 1.75–1.95 (m, 4H), 2.20 (s, 3H), 2.25–2.40 (m, 6H), 2.95 (t, 2H), 3.05 (t, 2H), 3.75 (s, 4H), 4.00 (t, 2H), 6.70–8.10 (m, 13H, Ar). ^{13}C NMR δ 23.47, 24.47, 25.99, 27.31, 27.33, 29.29, 27.27, 42.33, 54.61, 59.04, 61.45, 61.95, 68.02, 124.22, 126.82, 126.99, 128.24, 128.84, 129.31, 130.69, 133.63, 134.14, 135.14,

139.13, 139.24, 141.50, 142.23, 162.88, 186.79. MS (ES) *m/z*: 537 ($M+H^+$). Anal. $C_{36}H_{44}N_2O_2$ (C, H, N).

6.2. Inhibition of AChE and BuChE

The method of Ellman et al. was followed.[13] Five different concentrations of each compound were selected in order to obtain inhibition of AChE or BuChE activity comprised between 20% and 80%. The assay solution consisted of a 0.1 M potassium phosphate buffer pH 8.0, with the addition of 340 μM 5,5′-dithio-bis(2-nitrobenzoic acid), 0.02 unit/mL of human recombinant AChE or BuChE derived from human serum (Sigma Chemical), and 550 μM of substrate (acetylthiocholine iodide or butyrylthiocholine iodide, respectively). Test compounds were added to the assay solution and preincubated at 37 °C with the enzyme for 20 min followed by the addition of substrate. Assays were carried out with a blank containing all components except AChE or BuChE in order to account for non-enzymatic reaction. The reaction rates were compared, and the percent inhibition due to the presence of test compounds was calculated. Each concentration was analyzed in triplicate, and IC_{50} values were determined graphically from inhibition curves (log inhibitor concentration vs percent inhibition).

6.3. Inhibition of AChE-induced β-amyloid aggregation

Aliquots of 2 μL $A\beta_{40}$ peptide (Bachem AG, Germany), lyophilized from a 2 mg mL^{-1} HFIP (1,1,1,3,3,3-hexafluoro-2-propanol) solution and dissolved in DMSO, were incubated for 24 h at room temperature in 0.215 M sodium phosphate buffer (pH 8.0) at a final concentration of 230 μM. For co-incubation experiments aliquots (16 μL) of human recombinant AChE (final concentration 2.30 μM, Aβ/AChE molar ratio 100:1) and AChE in the presence of 2 μL of tested inhibitor (final concentration = 100 μM) were added. Blanks containing Aβ, AChE, and Aβ plus inhibitors, in 0.215 M sodium phosphate buffer (pH 8.0) were prepared. The final volume of each vial was 20 μL. Each assay was run in duplicate. To quantify amyloid fibril formation, the thioflavin T (ThT) fluorescence method was then applied.[22–24]

Analyses were performed with a Jasco Spectrofluorometer FP-6200 using a 3 mL quartz cell. After incubation, the samples containing Aβ, or Aβ plus AChE, or Aβ plus AChE in the presence of inhibitors were diluted with 50 mM glycine-NaOH buffer (pH 8.5) containing 1.5 μM thioflavin T to a final volume of 2.0 mL. A 300s-time scan of the emitted fluorescence (λ_{exc} = 446 nm, λ_{em} = 490 nm) was performed and the intensity values at the plateau were averaged after subtracting the background fluorescence of 1.5 μM thioflavin T and AChE.

The fluorescence intensities in the presence and in the absence of inhibitor were compared and the percentage of inhibition was calculated by the following expression: $100 - (IF_i/IF_o \times 100)$ where IF_i and IF_o are the fluorescence intensities obtained for Aβ plus AChE in the presence and in the absence of inhibitor, respectively.[22]

6.4. Determination of steady state inhibition constant

To obtain estimates of the competitive inhibition constant K_i, reciprocal plots of $1/v$ versus 1/[ATCh] were constructed at relatively low concentration of substrate (0.60–0.06 mM) and increasing inhibitor concentrations (range 0–50 nM). The plots were assessed by a weighted least square analysis that assumed the variance of v to be a constant percentage of v for the entire data set. Slopes of these reciprocal plots were then plotted against the concentration of **22** in a weighted analysis and K_i was determined as the intersect on the negative x-axis. Data analysis was performed with GraphPad Prism 4.03 software (GraphPad Software Inc.).

6.5. Inhibition of A_{42} self-aggregation

The spontaneous fibrilization of peptide $A\beta_{42}$ was investigated by a ThT-based fluorometric assay. HFIP (1,1,1,3,3,3-hexafluoro-2-propanol) pretreated $A\beta_{42}$ samples (Bachem AG, Switzerland) were resolubilized with a $CH_3CN/Na_2CO_3/NaOH$ (48.4:48.4:3.2) mixture to have a stable stock solution ([Aβ] = 500 μM).[25] Experiments were performed by incubating $A\beta_{42}$ in 10 mM phosphate buffer (pH 8.0) containing 10 mM NaCl, at 30 °C for 24 h (final $A\beta_{42}$ concentration = 50 μM) with and without the tested compound at 10 μM. To quantify amyloid fibril formation, the ThT fluorescence method was used.[23,24] After incubation, samples were diluted to a final volume of 2.0 mL with 50 mM glycine–NaOH buffer (pH 8.5) containing 1.5 μM thioflavin T. A 300-seconds-time scan of fluorescence intensity was carried out (λ_{exc} = 446 nm; λ_{em} = 490 nm), and values at plateau were averaged after subtracting the background fluorescence of 1.5 μM thioflavin T solution.% inhibition was calculated from the ratio between florescence intensities obtained in the presence and in the absence of inhibitor.

6.6. Computational studies

The molecular structure of human AChE was obtained from the Protein Data Bank (pdb accession code: 1b41).[26] The investigated compounds (**2**, **3**, **18**, and **19**) were build using the SYBYL 7.3 molecular modeling suite (Tripos Inc., St. Louis, MO), and each structure was optimized in the density functional theory (DFT) framework. All the DFT computations described in the text were carried out at the same level of theory (B3LYP/6-31G*) using the **gussian**03 software (Gaussian, Inc. Wallingford, CT). For the target, fasciculin and all water molecules were removed and the hydrogen atoms were added using the Biopolymer module of SYBYL. The ligand binding site was defined as 13 Å from the oxygen of Tyr124 side chain. Docking simulations were carried out using GOLD 3.0.1.[15] As suggested by the GOLD authors,[15] genetic algorithm default parameters were set: the population size was 100, the selection pressure was 1.1, the number of operations was 10^5, the number of islands was 5, the niche size was 2, migrate was 10, mutate was 95, and crossover was 95. For each compound, 100 poses were generated by GOLD and then clusterized by means of AClAP (v. 1.0).[16,17] Briefly, AClAP is a newly developed clustering protocol implemented in a MATLAB metalanguage program, which combines a hierarchical agglomerative cluster analysis with a clusterability assessment method and a user independent cutting rule. Several mathematical rules for both hierarchical tree construction and cutting are implemented in the algorithm. However, we have demonstrated that, when applied to docking outcomes, the combination of the average linkage rule with the cutting function developed by Sutcliffe and co-workers[27] turned out to be an approach that meets all of the criteria required for a robust clustering protocol.[16,17] The poses reported in Figure 1 are docking configurations representative of clusters statistically populated according to the Chaevenaut criterion, implemented in the code.[16,17] Notably, such poses were also low energy docking poses according to the GOLD scoring function.

References and notes

1. Harrison, P. J. *J. R. Soc. Med.* **1986**, *79*, 347–352.
2. Terry, A. V.; Buccafusco, J. J. *J. Pharmacol. Exp. Ther.* **2003**, *306*, 821–827.
3. Finder, V. H.; Glockshuber, R. *Neurodegener. Dis.* **2007**, *4*, 13–27.
4. Alvarez, A.; Opazo, C.; Alarcon, R.; Garrido, J.; Inestrosa, N. C. *J. Mol. Biol.* **1997**, *272*, 348–361.
5. De Ferrari, G. V.; Canales, M. A.; Shin, I.; Weiner, L. M.; Silman, I.; Inestrosa, N. C. *Biochemistry* **2001**, *40*, 10447–10457.
6. Bourne, Y.; Taylor, P.; Radić, Z.; Marchot, P. *EMBO J.* **2003**, *22*, 1–12.

7. Cavalli, A.; Bottegoni, G.; Raco, C.; De Vivo, M.; Recanatini, M. *J. Med. Chem.* **2004**, *47*, 3991–3999.
8. Greenblatt, H. M.; Dvir, H.; Silman, I.; Sussman, J. L. *J. Mol. Neurosci.* **2003**, *20*, 369–383.
9. Piazzi, L.; Rampa, A.; Bisi, A.; Gobbi, S.; Belluti, F.; Cavalli, A.; Bartolini, M.; Andrisano, V.; Valenti, P.; Recanatini, M. *J. Med. Chem.* **2003**, *46*, 2279–2282.
10. Belluti, F.; Rampa, A.; Piazzi, L.; Bisi, A.; Gobbi, S.; Bartolini, M.; Andrisano, V.; Cavalli, A.; Recanatini, M.; Valenti, P. *J. Med. Chem.* **2005**, *48*, 4444–4456.
11. Piazzi, L.; Cavalli, A.; Belluti, F.; Bisi, A.; Gobbi, S.; Rizzo, S.; Bartolini, M.; Andrisano, V.; Recanatini, M.; Rampa, A. *J. Med. Chem.* **2007**, *50*, 4250–4254.
12. Rizzo, S.; Cavalli, A.; Ceccarini, L.; Bartolini, M.; Belluti, F.; Bisi, A.; Andrisano, V.; Recanatini, M.; Rampa, A. *ChemMedChem* **2009**, *4*, 670–679.
13. Ellman, G. L.; Courtney, K. D.; Andres, V.; Featherstone, R. M. *Biochem. Pharmacol.* **1961**, *7*, 88–95.
14. Sugimoto, H.; Yamanishi, Y.; Rimura, Y.; Kawakami, Y. *Curr. Med. Chem.* **2000**, *7*, 303–339.
15. Jones, G.; Willet, P.; Glen, R. C.; Leach, A. R.; Taylor, R. *J. Mol. Biol.* **1997**, *267*, 727–748.
16. Bottegoni, G.; Cavalli, A.; Recanatini, M. *J. Chem. Inf. Model.* **2006**, *46*, 852–862.
17. Bottegoni, G.; Rocchia, W.; Recanatini, M.; Cavalli, A. *Bioinformatics* **2006**, *22*, e58–e65.
18. Sulpizi, M.; Carloni, P. J. *Phys. Chem. B* **2000**, *104*, 10087–10091.
19. Darvesh, S.; Hopkins, D. A.; Geula, C. *Nat. Rev. Neurosci.* **2003**, *4*, 131–138.
20. Greig, N. H.; Utsuki, T.; Ingram, D. K.; Wang, Y.; Pepeu, G.; Scali, C.; Yu, Q. S.; Mamczarz, J.; Holloway, H. W.; Giordano, T.; Chen, D.; Furukawa, K.; Sambamurti, K.; Brossi, A.; Lahir, D. K. *Proc. Natl. Acad. Sci.* **2005**, *102*, 17213–17218.
21. Bartorelli, L.; Giraldi, C.; Saccardo, M.; Cammarata, S.; Bottini, G.; Fasanaro, A. M.; Trequattrini, A. *Curr. Med. Res. Opin.* **2005**, *21*, 1809–1818.
22. Bartolini, M.; Bertucci, C.; Cavrini, V.; Andrisano, V. *Biochem. Pharmacol.* **2003**, *65*, 407–416.
23. Naiki, H.; Higuchi, K.; Nakakuki, K.; Takeda, T. *Lab. Invest.* **1991**, *65*, 104–110.
24. LeVine, H., 3rd *Protein Sci.* **1993**, *2*, 404–410.
25. Bartolini, M.; Bertucci, C.; Bolognesi, M. L.; Cavalli, A.; Melchiorre, C.; Andrisano, V. *ChemBioChem* **2007**, *8*, 2152–2161.
26. Kryger, G.; Harel, M.; Giles, K.; Toker, L.; Velan, B.; Lazar, A.; Kronman, C.; Barak, D.; Ariel, N.; Shafferman, A.; Silman, I.; Sussman, J. L. *Acta Crystallogr., Sect. D* **2000**, *56*, 1385–1394.
27. Kelley, L. A.; Gardner, S. P.; Sutcliffe, M. J. *Protein Eng.* **1997**, *10*, 737–741.
28. Savini, L.; Gaeta, A.; Fattorusso, C.; Catalanotti, B.; Campiani, G.; Chiasserini, L.; Pellerano, C.; Novellino, E.; McKissic, D.; Saxena, A. *J. Med. Chem.* **2003**, *46*, 1–4.
29. Branduardi, D.; Gervasio, F. L.; Cavalli, A.; Recanatini, M.; Parrinello, M. *J. Am. Chem. Soc.* **2005**, *127*, 9147–9155.
30. Petraglio, G.; Bartolini, M.; Branduardi, D.; Andrisano, V.; Recanatini, M.; Gervasio, F. L.; Cavalli, A.; Parrinello, M. *Proteins* **2008**, *70*, 779–785.